



## Testing of bulk radiation damage of n-in-p silicon sensors for very high radiation environments

K. Hara<sup>p,\*</sup>, A.A. Affolder<sup>h</sup>, P.P. Allport<sup>h</sup>, R. Bates<sup>e</sup>, C. Betancourt<sup>m</sup>, J. Boehm<sup>l</sup>, H. Brown<sup>h</sup>, C. Buttar<sup>e</sup>, J.R. Carter<sup>b</sup>, G. Casse<sup>h</sup>, H. Chen<sup>a</sup>, A. Chilingarov<sup>g</sup>, V. Cindro<sup>i</sup>, A. Clark<sup>d</sup>, N. Dawson<sup>m</sup>, B. DeWilde<sup>o</sup>, F. Doherty<sup>e</sup>, Z. Dolezal<sup>k</sup>, L. Eklund<sup>e</sup>, V. Fadeyev<sup>m</sup>, D. Ferrere<sup>d</sup>, H. Fox<sup>g</sup>, R. French<sup>n</sup>, C. García<sup>q</sup>, M. Gerling<sup>m</sup>, S. Gonzalez Sevilla<sup>d</sup>, I. Gorelov<sup>j</sup>, A. Greenall<sup>h</sup>, A.A. Grillo<sup>m</sup>, N. Hamasaki<sup>p</sup>, H. Hatano<sup>p</sup>, M. Hoeferkamp<sup>j</sup>, L.B.A. Hommels<sup>b</sup>, Y. Ikegami<sup>f</sup>, K. Jakobs<sup>c</sup>, J. Kierstead<sup>a</sup>, P. Kodys<sup>k</sup>, M. Köhler<sup>c</sup>, T. Kohriki<sup>f</sup>, G. Kramerberger<sup>i</sup>, C. Lacasta<sup>q</sup>, Z. Li<sup>a</sup>, S. Lindgren<sup>m</sup>, D. Lynn<sup>a</sup>, P. Maddock<sup>m</sup>, I. Mandić<sup>i</sup>, F. Martinez-McKinney<sup>m</sup>, S. Martí i Garcia<sup>q</sup>, R. Maunu<sup>o</sup>, R. McCarthy<sup>o</sup>, J. Metcalfe<sup>j</sup>, M. Mikestikova<sup>l</sup>, M. Mikuž<sup>i</sup>, M. Miñano<sup>q</sup>, S. Mitsui<sup>p</sup>, V. O'Shea<sup>e</sup>, U. Parzefall<sup>c</sup>, H.F.-W. Sadrozinski<sup>m</sup>, D. Schamberger<sup>o</sup>, A. Seiden<sup>m</sup>, S. Terada<sup>f</sup>, S. Paganis<sup>n</sup>, D. Robinson<sup>b</sup>, D. Poldon<sup>o</sup>, S. Sattari<sup>m</sup>, S. Seidel<sup>j</sup>, Y. Takahashi<sup>p</sup>, K. Toms<sup>j</sup>, D. Tsionou<sup>n</sup>, Y. Unno<sup>f</sup>, J. Von Wilpert<sup>m</sup>, M. Wormald<sup>h</sup>, J. Wright<sup>m</sup>, M. Yamada<sup>p</sup>

<sup>a</sup> Brookhaven National Laboratory, Physics Department and Instrumentation Division, Upton, NY 11973-5000, USA

<sup>b</sup> Cavendish Laboratory, University of Cambridge, JJ Thomson Avenue, Cambridge CB3 0HE, UK

<sup>c</sup> Physikalisches Institut, Universität Freiburg, Hermann-Herder-Str 3, D-79104 Freiburg, Germany

<sup>d</sup> Section de Physique, Université de Genève, 24, rue Ernest Ansermet CH-1211 Genève, Switzerland

<sup>e</sup> Department of Physics and Astronomy, University of Glasgow, Glasgow G12 8QQ, UK

<sup>f</sup> KEK, High Energy Accelerator Organization, INPS, 1-1 Oho, Tsukuba, Ibaraki 305-0801, Japan

<sup>g</sup> Physics Department, Lancaster University, Lancaster LA1 4YB, UK

<sup>h</sup> Oliver Lodge Laboratory, Department of Physics, University of Liverpool, Oxford St. Liverpool L69 7ZE, UK

<sup>i</sup> Jožef Stefan Institute and Department of Physics, University of Ljubljana, Ljubljana, Slovenia

<sup>j</sup> Department of Physics and Astronomy University of New Mexico, MSC07 4220 800 Yale Blvd. NE Albuquerque, NM 87131, USA

<sup>k</sup> Faculty of Mathematics and Physics, Charles University in Prague, V Holesovickach 2 Prague 8, Czech Republic

<sup>l</sup> Institute of Physics, Academy of Sciences of the Czech Republic, Na Slovance 2, 18221 Prague 8, Czech Republic

<sup>m</sup> SLIPP, UC Santa Cruz, CA 95064, USA

<sup>n</sup> Department of Physics and Astronomy, The University of Sheffield, Hicks Building, Hounsfield Road, S3 7RH Sheffield, U.K

<sup>o</sup> Department of Physics and Astronomy, Stony Brook University, Stony Brook, NY 11794-3800, USA

<sup>p</sup> School of Pure and Applied Sciences, University of Tsukuba, 1-1-1 Tennodai, Tsukuba, Ibaraki 305-8571, Japan

<sup>q</sup> IFIC (Centro Mixto CSIC-UVeG), Edificio Investigacion Paterna, Apartado 22085 46071 Valencia, Spain

### ARTICLE INFO

Available online 28 April 2010

#### Keywords:

p-Bulk silicon

Microstrip

Charge collection

Radiation damage

### ABSTRACT

We are developing n<sup>+</sup>-in-p, p-bulk and n-readout, microstrip sensors, fabricated by Hamamatsu Photonics, as a non-inverting radiation hard silicon detector for the ATLAS tracker upgrade at the super-LHC (sLHC) proposed facility. The bulk radiation damage after neutron and proton irradiations is characterized with the leakage current, charge collection and full depletion voltage. The detectors should provide acceptable signal, signal-to-noise ratio exceeding 15, after the integrated luminosity of 6000 fb<sup>-1</sup>, which is twice the sLHC integrated luminosity goal.

© 2010 Elsevier B.V. All rights reserved.

### 1. Introduction

The silicon microstrip detector continues to play an essential role in high-energy experiments for its capability for precision tracking. The detectors at the planned super-Large Hadron

Collider (LHC) are required to remain operational up to an integrated luminosity of 3000 fb<sup>-1</sup> with an instantaneous luminosity of  $1 \times 10^{35} \text{ cm}^{-2} \text{ s}^{-1}$ . In order to cope with this ten-fold increase in instantaneous luminosity beyond the design value of the LHC, currently under commissioning, the ATLAS collaboration is investigating an inner tracking system based fully on semiconductor devices. The segmentation will be varied in radius  $R$  with the innermost layers being pixels, followed by short (2.4 cm) and long (9.7 cm) microstrip detectors. The expected

\* Corresponding author.

E-mail address: [hara@hep.px.tsukuba.ac.jp](mailto:hara@hep.px.tsukuba.ac.jp) (K. Hara).

radiation fluence [1] including a safety factor of two is  $(7\text{--}11) \times 10^{14}$  1-MeV  $n_{\text{eq}}/\text{cm}^2$  for the short strip ( $R \geq 38$  cm) and  $(3\text{--}6) \times 10^{14}$  1-MeV  $n_{\text{eq}}/\text{cm}^2$  for the long strip ( $R \geq 85$  cm) regions, where the ranges within the parentheses are the highest fluence values at the central and forward regions, respectively. The charged particle contribution to the fluence is similar to the neutral at  $R \sim 28$  cm in the central region but decreases with  $R$  and in the forward region to typically 20% of the total. It is therefore important to investigate the damage due to both charged particles and neutrons.

The ATLAS R&D group “Development of non-inverting silicon strip detectors for the ATLAS ID upgrade” was formed to develop radiation hard tracking detectors based on p-bulk microstrips [2]. Since the radiation induced impurity in silicon contributes dominantly acceptor like states,  $n^+$ -on-p devices are non-inverting. N-strip readout allows us to operate the sensors at partial depletion, if required. However, the experience of employing p-bulk silicon for particle trackers is limited. This is in part because additional strip isolation structures are required for individual read-out strips to prevent electron accumulation between strips effectively shorting them together. The R&D group is evaluating sensors fabricated by Hamamatsu Photonics using commercially available p-type wafers. We report here on the bulk damage aspects, including the increase of leakage current, the decrease in charge collection (CC) and the full depletion voltage (FDV) evolution. The surface damage aspects are reported in Ref. [3].

## 2. Samples and irradiation

The sample sensors were fabricated using 15 cm wafers with  $\langle 100 \rangle$  crystal orientation and  $320 \mu\text{m}$  thickness. The new data we report on in this paper are float-zone grown wafers (FZp wafers in Ref. [4]), showing better leakage current characteristics than other p-type FZ wafers (FZs wafers in Ref. [4]) available to Hamamatsu. The initial FDV is 200 V. The R&D group continues to evaluate other commercially available p-type wafers including magnetic Czochralski grown wafers (MCZ in [4]). The strip pitch is  $74.5 \mu\text{m}$ . Details of the design, including strip isolation structures, are given in Ref. [2]. The performance of the main sensors,  $97.5 \text{ mm}$  square, is reported elsewhere [5]. The characteristics of irradiated sensors are studied using miniature samples of  $10 \text{ mm}$  square, where there are 100 strips of  $8 \text{ mm}$  length.

The proton irradiation was performed at Cyclotron Radio Isotope Centre (CYRIC) of Tohoku University. Details of the irradiation facility and methods are provided in Refs. [4,6]. The sample sensors were uniformly irradiated by 70-MeV protons through scanning them periodically in the beam. The irradiation took typically tens of minutes to a few hours depending on the fluence. The sensors were kept cold at  $-7^\circ\text{C}$  during irradiation and the irradiated samples were immediately stored in a refrigerator to prevent any post-irradiation annealing from taking place. The samples measured in Japan were glued onto a printed circuit board and biased at  $-100 \text{ V}$  during the irradiation. The samples measured outside Japan were irradiated as bare chips with no bias applied. The fluence we refer to is the 1-MeV neutron equivalent value, taking into account the non-ionising energy loss (NIEL) correction factor of 1.4. The fluence uncertainty is determined by the  $^{27}\text{Al}(\text{pn})$  reaction cross-section, which is no more than 10%.

The neutron irradiation was carried out at TRIGA reactor in Ljubljana, Slovenia [7]. The spectrum averaged NIEL factor is 0.88 with the overall fluence uncertainty of 10%. The irradiation was made at a rate of  $1.9 \times 10^{12} n_{\text{eq}} \text{ cm}^{-2} \text{ s}^{-1}$  with no bias to the sensors. The irradiation to  $10^{15} n_{\text{eq}} \text{ cm}^{-2}$  is thus completed in

9 min and annealing effect during irradiation can be ignored. The irradiated samples were stored in a refrigerator.

We compare the charge collection of Hamamatsu sensors with Micron sensors [8,9]. Micron samples were irradiated in addition using the 26-MeV protons at Compact Cyclotron, Karlsruhe and 24 GeV/c protons at CERN Proton Synchrotron.

## 3. Annealing

The irradiated sensors are known to show beneficial annealing, followed by degradation such as in reduced signal and FDV increase [10]. Fig. 1 shows the FDV evolutions measured with three samples [11], which were irradiated with protons to  $2 \times 10^{14} n_{\text{eq}} \text{ cm}^{-2}$ . The data for two neutron irradiated FZp samples are shown in Fig. 2. Both proton and neutron data are consistent with a FDV minimum after around 80 min at  $60^\circ\text{C}$ , which is similar to the annealing curves measured for n-bulk sensors [10].

## 4. Leakage current

The leakage currents of proton irradiated sensors are plotted in Fig. 3 as a function of the bias voltage. The samples were annealed

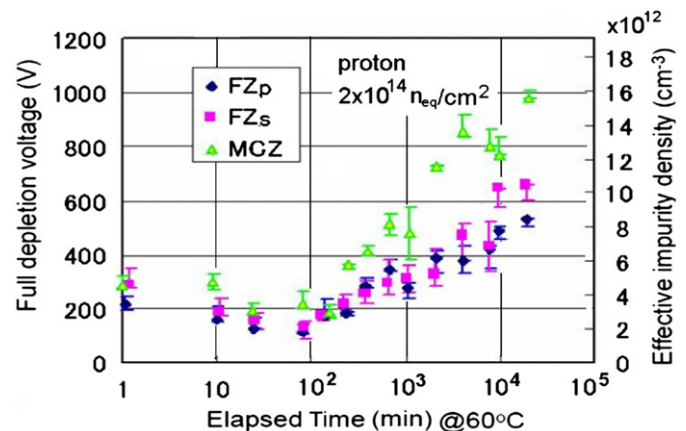


Fig. 1. Evolution of full depletion voltage as a function of annealing time, with samples kept at  $60^\circ\text{C}$ . The full depletion was determined from C-V curves and charge collection curves to infrared laser [4]. These samples were irradiated with 70-MeV protons to  $2 \times 10^{14}$  1-MeV  $n_{\text{eq}}/\text{cm}^2$ .

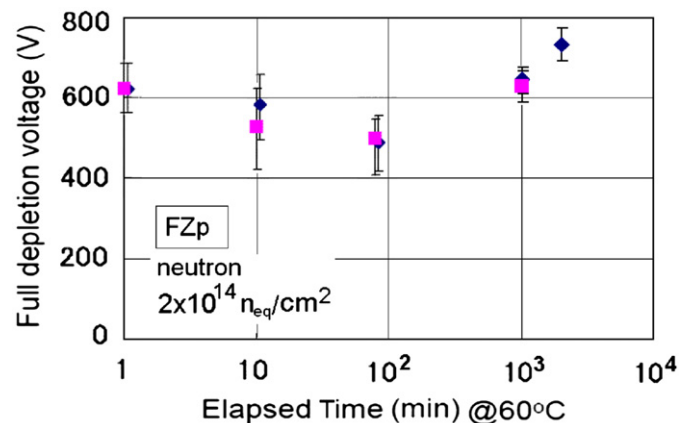


Fig. 2. Evolution of full depletion voltage of two FZ samples (irradiated with neutrons to  $2 \times 10^{14}$  1-MeV  $n_{\text{eq}}/\text{cm}^2$ ) as a function of annealing time, with samples kept at  $60^\circ\text{C}$ . The full depletion was determined from C-V curves and charge collection curves to  $^{90}\text{Sr}$   $\beta$ -ray.

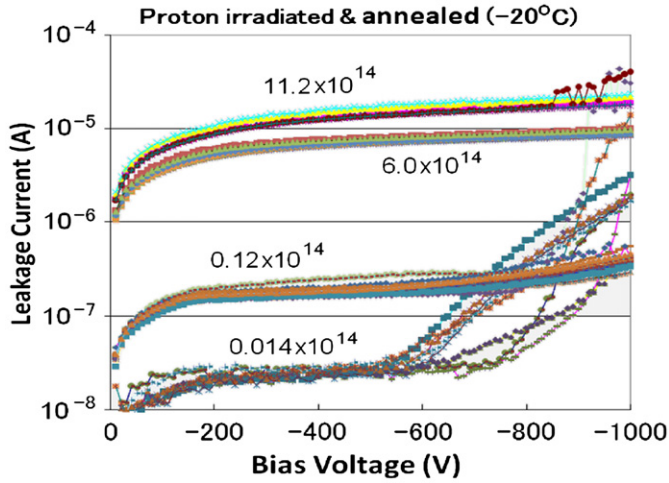


Fig. 3. Leakage current vs bias voltage of the samples irradiated with protons. The numbers attached to the curves are the charged particle fluence corrected to  $n_{eq}/cm^2$ .

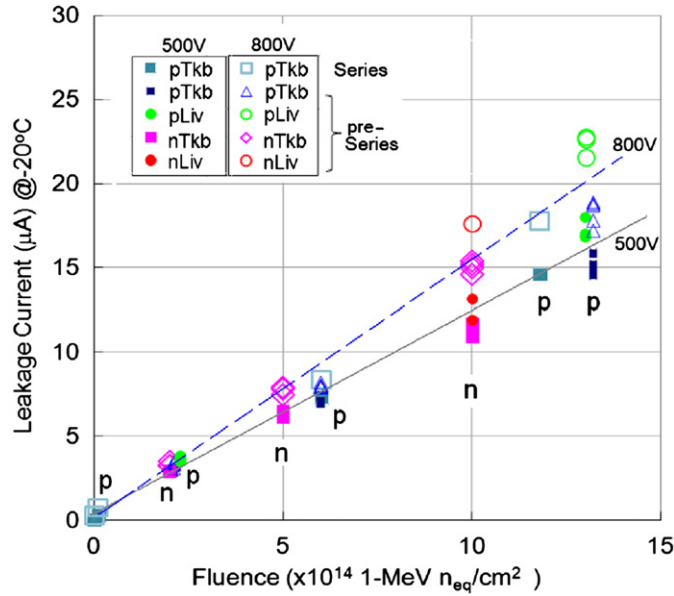


Fig. 4. Leakage current at (filled marks) 500 V and (open) 800 V irradiated with protons and neutrons (p or n attached). The lines are drawn to guide the eye. The samples are from two productions.

for 80 min at 60 °C. The temperature during the measurement is  $-20$  °C. The fluence ranged from  $1.4 \times 10^{12}$  to  $1.12 \times 10^{15}$  1-MeV  $n_{eq}/cm^2$ . The leakage current increase seen at the lowest fluence is not consistent with micro-discharge [12], and is understood as resulting from surface current. The increase disappears for the samples irradiated to  $10^{13}$   $n_{eq}/cm^2$  and above.

The leakage current values at 500 and 800 V are plotted in Fig. 4 for proton and neutron irradiated samples. We note that there is little difference between proton and neutron irradiations. The damage constant known for n-bulk,  $(3.99 \pm 0.03) \times 10^{-17}$  A/cm [10], can be translated to  $17.3$   $\mu$ A at  $10^{15}$  1-MeV  $n_{eq}/cm^2$  for effective area of  $80$  mm<sup>2</sup> and  $0.32$  mm thickness. Here the energy gap of  $1.12$  eV is taken for the temperature correction. The measured values are in reasonable agreement taking into account that the FDV is approximately  $700$  V. We conclude that the p-type wafers exhibit a damage constant similar to that of n-type wafers. We note that FZp wafers show a pre-irradiation leakage current similar to that of Hamamatsu n-bulk sensors.

## 5. Charge collection (CC)

### 5.1. Measurement system and requirement in CC

The charge collection (CC) resulting from penetrating  $^{90}\text{Sr}$   $\beta$ -rays was evaluated at four sites independently using different systems. The Liverpool and Ljubljana groups employed an analogue electronics chip (SCT128) [13] clocked at  $40$  MHz that has  $25$  ns shaping time. The Valencia group has used the LHCb “Beetle” ASIC [14] with analogue signal output. Conventional discrete amplifiers ( $10$  ns peaking time) and CAMAC ADC system were used by the Tsukuba/KEK group. These groups define the collected charge as the most probable charge of the analogue signal distributions. The UCSC group had a binary readout system based on PTSM ( $100$  ns shaping time) [15]. In all the sites the samples were cooled to  $-20$  to  $-30$  °C and scintillation counters were used for triggering. Fig. 5 shows that the charge collection of non-irradiated samples is consistently measured at four of the sites.

The electronics noise of the new  $250$  nm ABCN chips [16], which is the first version of the readout ASIC planned for use for the ATLAS strip upgrade is under evaluation [17,18]. The measurements indicate a noise of around  $600$  ENC for short strip and of  $950$  ENC for long strip sensors. In order to re-use the present ATLAS infrastructure, mainly the cables, it is preferred that reasonable signal-to-noise ratio ( $S/N > 10$ ) be achieved at maximum rated voltage of  $500$  V bias. Taking into account the maximum fluence, including a safety factor of two, the collected charge is required to be larger than  $6$  ke<sup>-</sup> at  $10^{15}$   $n_{eq}/cm^2$  (short strips) and  $9.5$  ke<sup>-</sup> at  $6 \times 10^{14}$   $n_{eq}/cm^2$  (long strips) at  $500$  V bias in order to achieve  $S/N > 10$ .

### 5.2. Annealing in CC curve

The charge collection of the irradiated samples was measured either with or without annealing. We studied the change in CC curves due to annealing in order to compare the results from all sites. Fig. 6 shows that two samples irradiated with protons to  $1.12 \times 10^{15}$  1-MeV  $n_{eq}/cm^2$  exhibited identical CC before annealing, and  $10$ – $30\%$  larger CC after annealing for  $80$  min at  $60$  °C. The CC for the samples irradiated with neutrons to  $2 \times 10^{14}$  and  $5 \times 10^{14}$  1-MeV  $n_{eq}/cm^2$  showed also an increase of  $10$ – $30\%$ , as shown in Fig. 7.

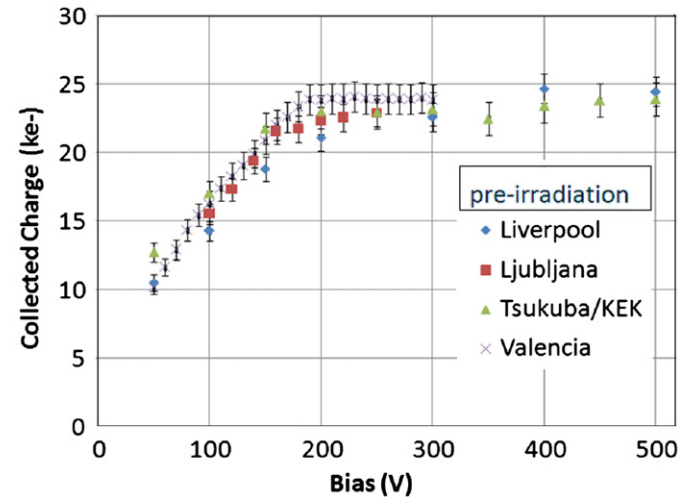


Fig. 5. Charge collection in kilo-electrons of non-irradiated samples, measured independently at four sites.

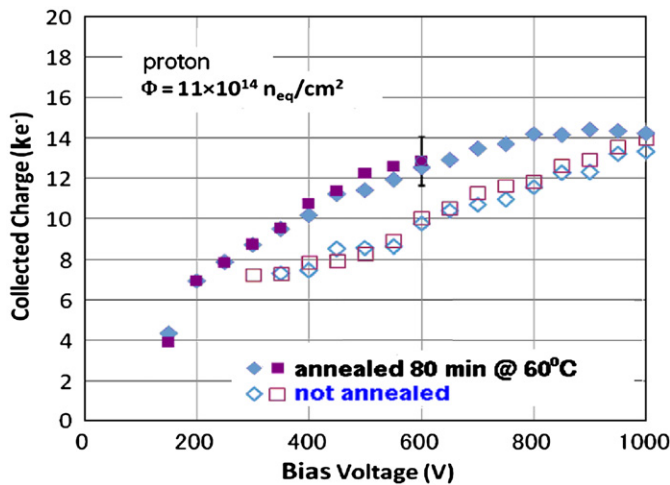


Fig. 6. Charge collection measured before (open marks) and after (filled) the annealing of 80 min at 60 °C. The two samples were irradiated with protons to  $1.12 \times 10^{15}$  1-MeV  $n_{eq}/cm^2$ . Typical uncertainty is shown as an error bar.

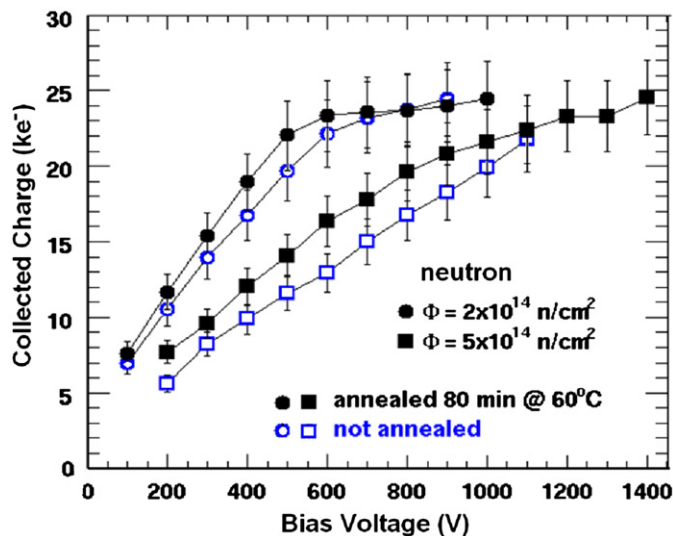


Fig. 7. Charge collection measured before (open marks) and after (filled) annealing. The two samples were irradiated with neutrons to  $2 \times 10^{14}$  and  $5 \times 10^{14}$  1-MeV  $n_{eq}/cm^2$ .

In the following comparisons, we multiply by 1.2 the CC data measured without annealing in order to emulate the effects of annealing.

### 5.3. Charge collection of proton irradiated samples

Fig. 8 shows the CC of proton irradiated samples measured at various sites. The two plots are approximately for the expected maximum fluence for the short and long strip sensors. The horizontal bars correspond to the  $S/N=10$  criteria for short and long strip sensors. In both cases, however,  $S/N$  of 18–20 should be achievable at 500 V.

### 5.4. Charge collection of neutron irradiated samples

Fig. 9 shows the CC corresponding measurements for neutron irradiated samples. The two plots correspond approximately to

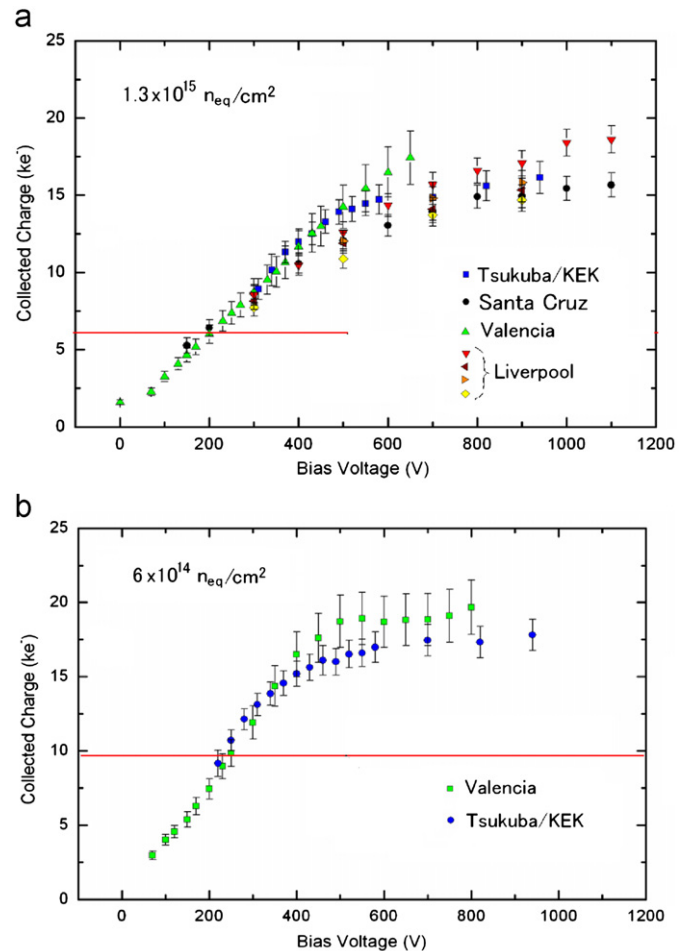


Fig. 8. Charge collection of proton irradiated samples: (top)  $1.3 \times 10^{15}$  and (above)  $6 \times 10^{14}$  1-MeV  $n_{eq}/cm^2$ . The horizontal bars correspond to  $S/N=10$  (see text).

the maximum expected fluence for the short and long strip sensors. The horizontal bars correspond to the  $S/N=10$  criteria for short and long strip sensors. In both cases,  $S/N$  of 15–18 should be achievable at 500 V.

### 5.5. Comparison with other strip detectors

The charge collection of various sensor types fabricated by Micron has been evaluated by Liverpool group [8,9]. The collected charge at 500 V bias is shown in Fig. 10, together with the present data for Hamamatsu sensors. Since no annealing was included in the Micron data, the collected charge from the previous plots (Figs. 8 and 9) was reduced by  $20 \pm 10\%$  for direct comparison. Among these, the p-in-n sensors show much lower CC for both FZ and MCz bulk material. The FZ n-side read-out sensors from Hamamatsu and Micron are similar both for proton and neutron irradiations.

### 5.6. Dependence on irradiation sources

Fig. 11 shows the collected charge of Hamamatsu and Micron  $n^+$ -in-p FZ sensors at 500 V bias for various irradiation sources. The Micron data are from [9] and the Hamamatsu data correspond to the condition without annealing. At 500 V, the differences are small between the different irradiation sources.



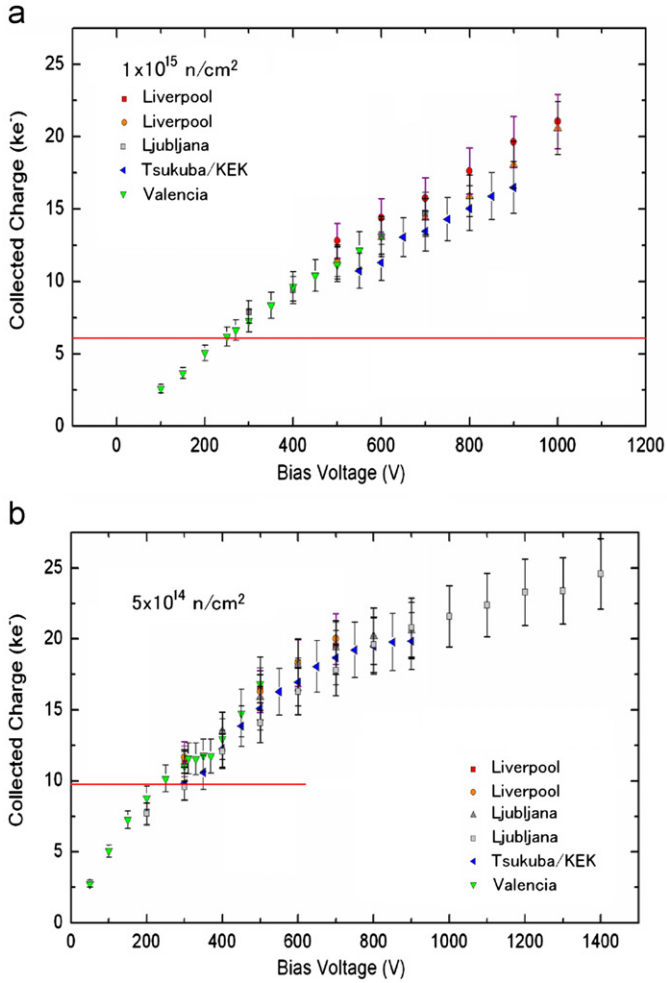


**Fig. 9.** Charge collection of neutron irradiated samples: (top)  $1 \times 10^{15}$  and (above)  $5 \times 10^{14}$   $1\text{-MeV } n_{\text{eq}}/\text{cm}^2$ . The horizontal bars correspond to  $S/N=10$  (see text).

## 6. Full depletion voltage

The full depletion voltage (FDV) is an important parameter for detector operation, although sufficient signal charge can be collected even under partial depletion.

The FDV is evaluated from the bulk capacitance  $C$ – $V$  characteristics ( $f_{\text{LCR}}=1\text{ kHz}$ ) and from the charge collection  $CC$ – $V$  curves. Examples are shown in Fig. 12 for two proton fluence values: (a)  $1.2 \times 10^{13}$  and (b)  $1.1 \times 10^{15}$   $n_{\text{eq}}/\text{cm}^2$ . At  $1.2 \times 10^{13}$ , the  $C$ – $V$  curves exhibit characteristic distortions for the samples with p-stop only while samples with p-spray in addition show good agreement with the curve expected from  $CC$ – $V$ . Note that  $CC$ – $V$  is consistent between the two sample groups.

The above distortion was observed only at  $1.2 \times 10^{13}$   $n_{\text{eq}}/\text{cm}^2$ . Non-linear dependence in  $1/C^2$  curves, as shown in Fig. 12b, becomes more distinct at larger fluence. The  $CC^2$ – $V$  curve, however, increases linearly with the bias as expected.

The FDV is defined from the  $CC^2$ – $V$  curve as the bias where the linear line intercepts with the saturated plateau. At the highest fluence, where the plateau is not obvious, the plateau is taken as the one derived from the lower fluence data. The FDV from  $1/C^2$ – $V$  is determined similarly but two lines defined in lower and higher bias ranges are used and the difference was taken as the uncertainty. The central FDV value is taken as the one derived from the lower bias range.

The FDV is summarized in Fig. 13 as a function of the fluence for proton and neutron irradiated samples. The agreement

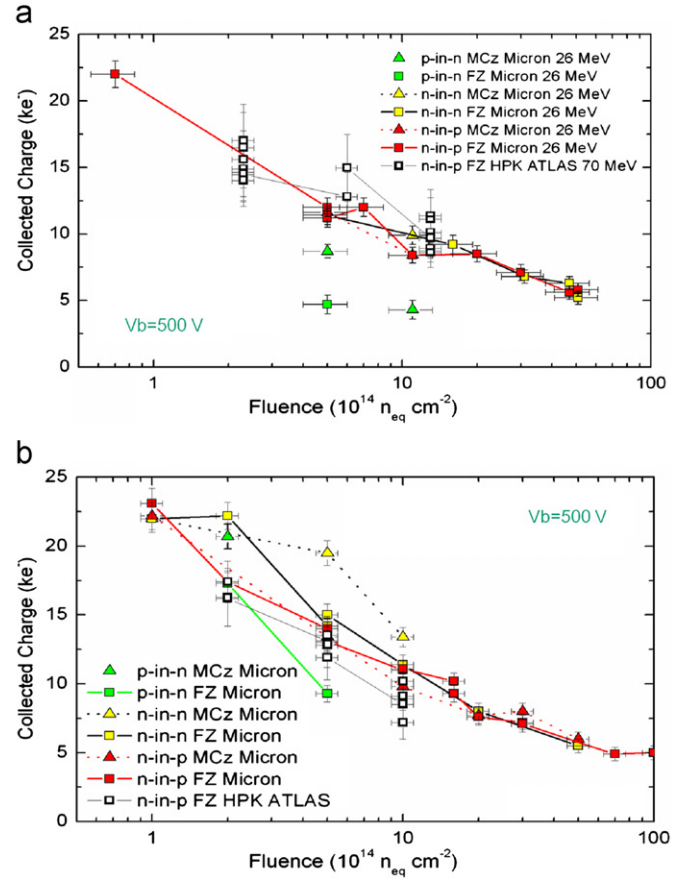


**Fig. 10.** Charge collection at 500 V bias in comparison with Micron sensors: (top) proton irradiated samples and (above) neutron irradiated samples. Hamamatsu data are shown in open squares. See text for annealing corrections.

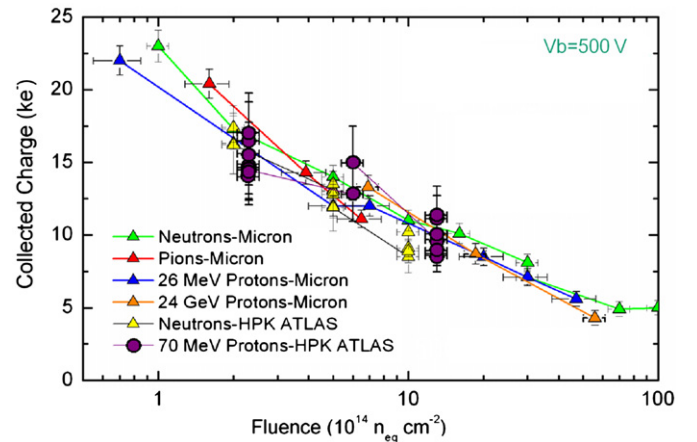


**Fig. 11.** Charge collection at 500 V of Hamamatsu and Micron FZ sensors for various types of irradiation sources. See text for annealing.

between  $C$ – $V$  and  $CC$ – $V$  is noticeable but the FDV differs between neutron and proton irradiations.

The difference in  $CC$ – $V$  curves between proton and neutron irradiation is shown in Fig. 14 where the charge collection is compared between two proton and two neutron irradiated samples. The fluence is similar,  $5 \times 10^{14}$  for neutrons and  $6 \times 10^{14}$   $n_{\text{eq}}/\text{cm}^2$  for protons, and all the samples were processed for the same annealing. Although the collected charge is similar at 500 V, it increases further with the bias for the neutron irradiated samples.

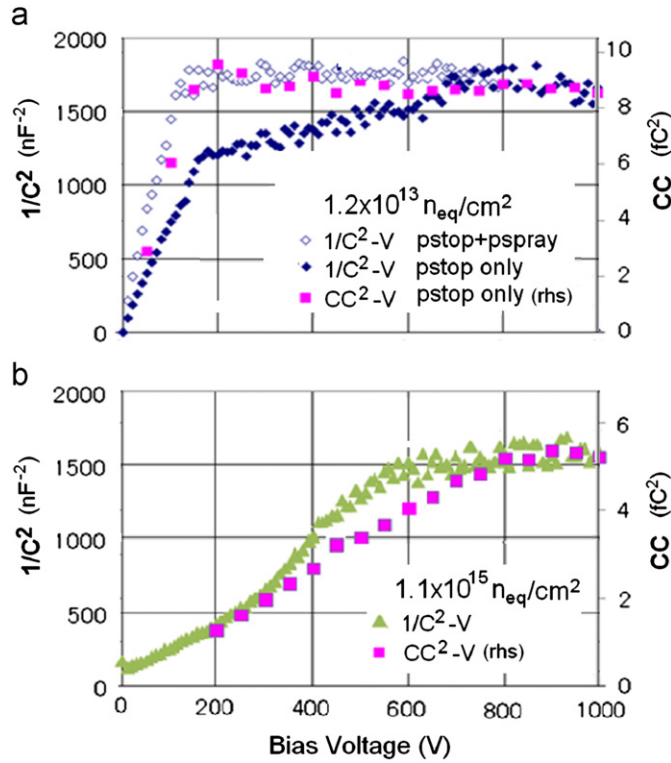


**Fig. 12.**  $1/C^2$  (lhs) and  $CC^2$  (rhs) vs bias voltage for the samples irradiated with protons to: (a)  $1.2 \times 10^{13}$  and (b)  $1.1 \times 10^{15}$   $n/cm^2$ . In (a)  $1/C^2$ -V curves for two samples are shown.

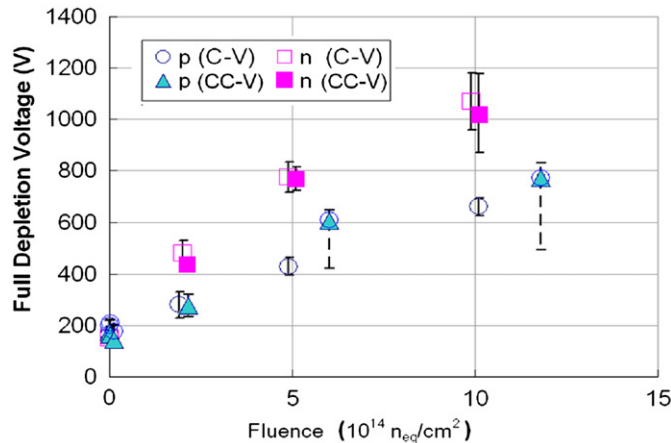


**Fig. 13.** Full depletion voltage as a function of the fluence for proton and neutron irradiated Hamamatsu FZ samples.

## 7. Summary

We are designing radiation hard silicon microstrip detectors for the ATLAS inner detector upgrade at the super LHC. P-bulk sensors are good candidates for such a very high radiation environment, reaching  $1 \times 10^{15}$  1-MeV  $n_{eq}/cm^2$ .

We evaluated the performance of Hamamatsu FZ grown samples irradiated with protons and neutrons. The leakage current increase and annealing property are in agreement with the characteristics known for n-bulk sensors.

The collected charge was measured with different systems using penetrating  $\beta$ -rays. At 500 V bias, the collected charge was similar for the neutron and proton irradiations, and also similar to

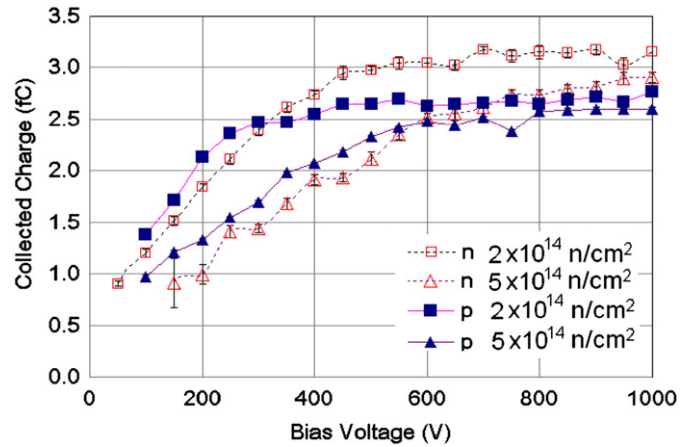


**Fig. 14.** Collected charge as a function of bias voltage for proton irradiated samples in comparison with neutron irradiated samples. There is an overall scale uncertainty of 5%. The sensors were annealed for 80 min at 60 °C before measurement.

results previously obtained from FZ sensors produced by Micron. Signal-to-noise ratio of 18–20 and 15–18 should be achievable for short and long strip sensors, respectively, at the maximum fluence where a safety factor of two is included.

The full depletion voltage extracted from capacitance–voltage studies rises at  $1 \times 10^{15}$   $n_{eq}/cm^2$  to  $\sim 700$  V for proton irradiation and to nearly 1 kV for neutron irradiation. Operation in partial depletion is therefore foreseen.

## Acknowledgements

We would like to acknowledge K. Yamamura and S. Kamada of Hamamatsu Photonics K.K. for fruitful discussions on sensor design. The teams of CYRIC, Tohoku University, Reactor Centre of Jožef Stefan Institute, Karlsruhe and CERN-PS are also acknowledged for conducting excellent irradiations. The research was partly supported by Ministry of Education, Youth and Sports of the Czech Republic, the German Federal Ministry of Education and Research, the Japan Grant-in-Aid for Scientific Research (A) (Grant no. 20244038), (C) (Grant no. 20540291), and on Priority Area (Grant no. 20025007), the UK Science and Technology Facilities Council (under Grant PP/E006701/1), and the US National Science Foundation (under Grant PHY0652607).

## References

- [1] I. Dawson, Radiation predictions at the SLHC and irradiation facilities, in: ATLAS Tracker Upgrade Workshop, Liverpool, 6–8 December 2006, <<http://www.liv.ac.uk/physics/AHLUTW/>>.
- [2] Y. Unno, et al., Development of n-on-p silicon sensors for very high radiation environment, this issue.
- [3] S. Lindgren, et al., Testing of surface properties pre-rad and post rad of n-in-p silicon sensor for very high radiation environment, this issue.
- [4] K. Hara, et al., IEEE Trans. Nucl. Sci. NS-56-2 (2009) 468.
- [5] M. Miestikova, et al., Testing of large area n-in-p silicon sensors intended for very high radiation environment, this issue.
- [6] Y. Unno, et al., Nucl. Instr. and Meth. A 579 (2007) 614.
- [7] D. Zontar, V. Cindro, et al., Nucl. Instr. and Meth. A 426 (1999) 51.
- [8] A. Affolder, et al., Nucl. Instr. and Meth. A 604 (2009) 250.
- [9] A. Affolder, P.P. Allport, G. Casse, in: Proceedings of the First International Conference on Technical Instrumentation in Particle Physics (TIPP09), Tsukuba, 12–17 March 2009, in press.
- [10] G. Lindstroem, et al., Nucl. Instr. and Meth. A 466 (2001) 308.
- [11] K. Hara et al., Characteristics of the irradiated Hamamatsu p-bulk silicon microstrip sensors, in: Proceedings of IEEE Nuclear Science Symposium, Dresden, Germany, October 19–25, 2008.
- [12] T. Ohsugi, et al., Nucl. Instr. and Meth. A 383 (1996) 166.
- [13] F. Anghinolfi, et al., IEEE Trans. Nucl. Sci. NS-44 (3) (1997) 298.
- [14] S. Löchner, M. Schmelling, The Beetle Reference Manual, LHCb-2005-105.

- [15] H.F.W. Sadrozinski, et al., IEEE Trans. Nucl. Sci NS-51-5 (2004) 2033.
- [16] J. Kaplon, et al., The ABCN front-end chip for ATLAS inner detector upgrade, in: Proceedings of Topical Workshop on Electronics for Particle Physics, TWEPP-08, Naxos, Greece, 15–19 September 2008, CERN-2008-0008 (2008) p. 116.
- [17] P.P. Allport, et al., Progress with the single-sided module prototypes for the ATLAS tracker upgrade stage, this issue.
- [18] Y. Ikegami, et al., Development of low-mass, high-density hybrid for the silicon microstrip sensors in very high radiation environment, this issue.